# 4 Tremor Frequency: The Source

Compared with the seismograms produced by the explosion and double-couple sources of earthquake seismology, volcanic tremor, especially harmonic tremor, is an unusual seismic signal. Earthquake sources, which are limited in time, are usually modeled as modified delta or step functions resulting from a dislocation in the earth. Seismic waves from the source then propagate through the earth. While the resulting seismogram may last for several hours depending on the epicentral distance, the frequency content of each segment is different and can be explained as a convolution of the source signal with the transfer function of the earth for the various types of waves. Harmonic tremor, on the other hand, continues for several hours at a time with only small changes in the frequency of the fundamental. It appears to be a sequence of repetitions of a slowly changing waveform. The changes in the shape of the waveform are reflected in the variation of the fundamental frequency, the amplitude, the frequency content and the polarization. An important objective of volcano seismology must be the effort to use information derived from tremor seismograms to describe the physical or chemical conditions at the tremor source through modelling.

Narrowband peaks observed in seismic recordings from volcanoes, particularly when they are members of a harmonic series, are generally attributed to oscillations of bodies of fluid or gas in the volcano. Several such models have been proposed, for instance, free eigenvibrations of a magma volume [Shima, 1958, Shimozuru, 1961], standing waves in a gas-filled conduit [Schlindwein et al, 1995, Benoit and McNutt, 1997] or the resonance of fluid-filled cracks [Mori et al, 1989 and Chouet, 1996]. In these models, the authors assume that the conduit and its contents are an oscillator which they describe using a linear differential equation and which has been excited by the action of an impulsive force of unspecified origin. They claim that any harmonic overtones observed are the result of the excitation of higher modes. For these models, the authors match the frequency of the oscillations to the frequency of the tremor by varying the dimensions of the conduit model, along with the density, viscosity and other characteristics of the fluid in the conduit. In fact, these models neglect the most interesting question in volcano seismology: what is the the physical process which provides the force to excite the oscillator?

The observations derived from Lascar's unusual harmonic tremor with many overtones provide a foundation on which to develop physical models for the tremor source process which go beyond the oscillations in a gas-filled volume or a fluid-filled body in response to an outside force. To produce a spectrum with many exactly integer harmonics as in Lascar's harmonic tremor, the seismic waves generated by the source must have extremely steep slopes and a well-defined periodicity, as do sawtooth or square waves. Waves with such characteristics have been recorded during the resonance of bubbles in a sound field [Leighton, 1994] and in shock waves during flow [Lighthill, 1993]. They have also been observed in cyclic and reversible phenomena with rapid transitions between two or more quasi-steady states like Trevelyan's rocker [Rayleigh, 1945]. Julian [1994] models the source for tremor with harmonic overtones as the movement of conduit walls in response to unsteady flow of magma. Thus, the characteristics of harmonic tremor suggest that it is caused by the flow of liquids or gases and their interaction with the conduit.

Changes in the fundamental frequency of the harmonic tremor also provide clues to characteristics of the source. While they might be produced by a change in the speed of sound along the propagation path, such a change is not likely to occur over an interval of seconds. Doppler shifting of a constant frequency source due to motion toward or away from the stations can also be excluded as a cause of the frequency changes, since the stations lie in different directions from the volcano. In addition, if the frequency changes were caused by Doppler shifting, the frequency should revert to the original, constant frequency after motion ends. The frequency changes are probably the result of some systematic change at the source.

Models for the source of harmonic tremor must produce waveforms with the following characteristics.

- The signals must have a well-defined periodicity and steep slopes at some point during the cycle. The steep slope causes the many harmonic lines in the Fourier amplitude and power spectra.
- The model must also allow the cycle length to change over the time frame of minutes, as can be observed in Figure 2.12.

- The process must be “non-destructive”, since it continues for hours with no apparent external effect on the volcano.

Many of the flow processes studied in fluid dynamics satisfy these criteria. They are repetitive and may continue for hours, as long as the reservoir of fluid at the source is large. There are several fluids in any active volcano which may be involved in flow processes: Magma, water, either in the form of liquid or steam, and other gases such as $CO_2$ and $SO_2$. In general, a flow regime is described by the Reynolds number, which is dimensionless,

$$Re = vd/\kappa, \qquad (4.1)$$

where $v$ is the flow velocity of the fluid, $d$ a measure of the characteristic dimension of the flow. $\kappa$, the kinematic viscosity of the fluid is defined as its shear or dynamic viscosity, $\eta$, divided by its density, $\rho$. The characteristic dimension of the flow regime depends on the specific example. In cases of flow in a conduit, $d$ is taken to be the conduit diameter, while it may be the diameter of an obstruction in other cases.

Three flow regimes in which a continuous, steady flow is converted into a cyclic stream can be modelled as Vortex Shedding, Slug Flow and the Soda Bottle. The three models can be distinguished on the basis of the range of Reynolds numbers in which they occur. Vortex shedding occurs when the Reynolds numbers lies between 100 and $10^5$ [Faber, 1995]. Slug flow begins in model flow systems if the Reynolds number rises above 2300 [Faber, 1995], while the Reynolds numbers for the Soda bottle model must be very low, on the order of 1 [Ginzburg, 1963]. For each of the three models, I describe the phenomenon and draw parallels between the experimental conditions under which it is observed and realisitic situations in a volcano which might produce it. Finally, I will constrain the model of the flow system using parameters measured from the harmonic tremor seismograms and discuss its implications for the source of tremor.

## 4.1 Vortex Shedding

Vortices or eddies often develop in the flow field, or wake, behind bluff objects. Two everyday phenomena caused by vortex shedding are the fluttering of a flag and the “singing“

of power lines in the wind. Fluid dynamics studies mainly concern themselves with the behavior of vortices behind cylinders, however vortex shedding has also been observed during flow past corners [Birkhoff and Zarantonello, 1957] or steps [Hogan and Morkovin, 1974] and in many other configurations which are important in engineering problems.

As the flow velocity increases, eddies which develop behind an object are likely to detach from it, forming a von Kármán vortex street. As each vortex develops and detachs, it produces sound waves. As long as the Reynolds number remains constant, eddies are shed regularly with alternating spin or vorticity. The sound pulses then appear as periodic oscillations of a sound field with a characteristic frequency [Morse and Ingard, 1968].

When the Reynolds number is low ($Re$ < 10), viscous forces are very important in a flow system. A fluid will flow smoothly and evenly around an object. As the velocity of the fluid, and consequently $Re$, increase, the flow separates from the object and eddies begin to develop on its downstream side. In calculating the Reynolds number, the characteristic dimension, $d$, is the diameter of the object. At still higher velocities ($Re$ > 100), the eddies

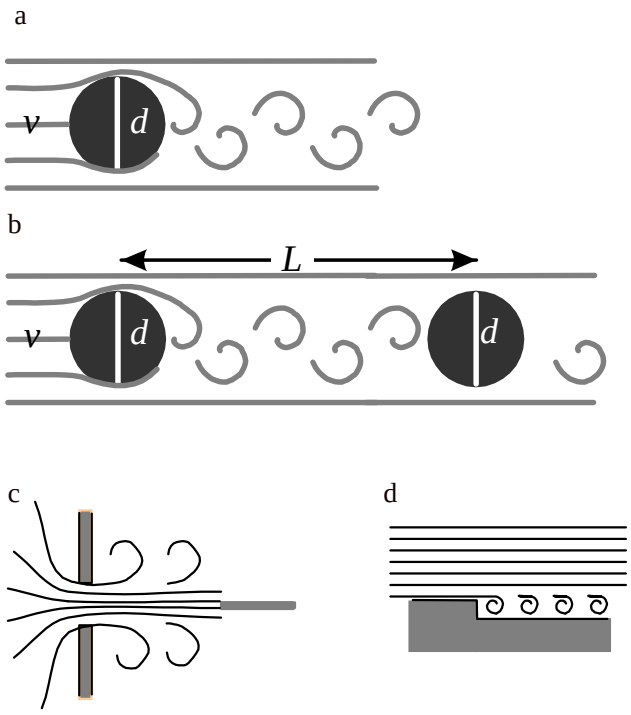


Figure 4.1 Model systems for eddy shedding. (a) Simple eddy shedding behind an obstacle. (b) Eddy shedding with resonance. (c) Jet edge whistle. (d) Eddies behind a step.

are shed regularly and a von Kármán vortex street develops (Figure 4.1). The shedding frequency, $f_K$, is given by the Strouhal number,

$$St = f_K\, d/v\ . \qquad (4.2)$$

In this case, the Reynolds and Strouhal numbers are calculated using the size of the obstacle for $d$. For all practical purposes, $St$ can be taken to be 0.2 when the Reynolds number lies between $10^2$ and $10^5$ [Morse and Ingard, 1968, Faber, 1995, Tritton, 1988]. When $Re$ > 1000, the wake becomes increasingly turbulent and the periodicity is less strong [Birkhoff and Zarantonello, 1957].

Under certain conditions vortex shedding may be coupled into a feedback mechanism, producing very large forces and sound amplitudes. As many as 10 integer harmonics have been observed [Morse and Ingard, 1968]. The geometric conditions necessary for stimulated sound emission due to a feedback resonance from eddy shedding exist when the shedding frequency, $f_K$, is equal to one of the transverse resonance frequencies of the duct, $f_i$. If there is a cylinder of diameter $d$ in a duct with the transverse dimension $D$, for example,

$$f_K = 0.2v/d = nc/2D = f_i, \quad i = 1, 2, 3, \ldots \qquad (4.3)$$

where $c$ is the speed of sound in the fluid.

Resonance may also occur when the vortex street produced by one cylinder interacts with a cylinder downstream (Figure 4.1b). The interaction between the eddies and the second cylinder produces a pressure disturbance which is radiated in all directions and propagates through the fluid with the velocity of sound. When the pressure pulse reaches the upstream cylinder, it affects the formation and detachment of the eddies. If the pressure disturbance arrives at the time in the formation cycle of a new vortex to stimulate its growth, the vortex will be amplified, and strong acoustic emission will result. To calculate the conditions necessary for stimulation, it is necessary to know how long it takes a vortex to travel between the two cylinders. If the cylinders are separated by a distance, $L$, a vortex reaches the second cylinder after an interval, $T_D = L/v_D$, where the eddy drift velocity, $v_D \sim 0.8v$ [Morse and Ingard, 1968]. The pressure pulse then travels at velocity $c$ back to the first

cylinder, and arrives there after an interval, $T_c = L/c$. Usually, $v_D \ll c$, so $T_D \gg T_c$ and the travel time of the pressure pulse can be ignored. The condition for resonance is then that the inverse of the travel time be a multiple of the von Kármán vortex frequency:

$$1/T_D = nf_K \qquad (4.4a)$$

or

$$v_D/L \sim 0.8v/L \ = 0.2nv/d, \text{ or } L \sim 4d/n. \qquad (4.4b)$$

Resonances with this type of geometry have produced damage in cooling towers of power plants [TRITTON, 1988].

Eddies form behind almost any object, not only cylinders, under the right flow conditions. HOGAN and MORKOVIN [1974] observed vortex formation at 9.5 Hz behind a 0.0013 m step with flow velocities in air of 3.3 m/s (Figure 4.1d). Vortex resonance can also be observed in jets (Figure 4.1c, [BIRKHOFF and ZARANTONELLO, 1957, MORSE and INGARD, 1968]). There are many reports of vibration-induced damage in dams [i.e. DOUMA, 1974, LYSSENKO and CHEPAJKIN, 1974, GONCHAROV and SEMENKOV, 1974]. In particular, LJATKHER [1980] describes “self-induced vibrations” in a dam spillway that he attributes to vortex shedding. The amplitude of these vibrations in an instrumented structure more than 2.5 km from the dam was greater than 0.5 mm/s.

In a volcano, it is unrealistic to expect to find cylinders in the center of a flow field. Steps, corners and jets similar to those sketched in Figure 4.1 are however not unlikely. Jets, for example, have been observed in association with steam explosions and harmonic events at Semeru [HELLWEG et al, 1994, SCHLINDWEIN et al, 1995]. In geological investigations of dike structures, junctions and constrictions have been observed which could act like corners or steps in a flow field.

Just as the fundamental frequency is a basic characteristic of harmonic tremor, von Kármán vortex streets, which occur when $10^2 < Re < 10^5$, are defined by their shedding frequency, $f_K$, (Equation 4.2). Solving Equations 4.1 and 4.2 for the flow velocity $v$ in terms of frequency, the Reynolds number and the kinematic viscosity gives:

$$v^2 = f_K \kappa Re/St. \qquad (4.5)$$

Figure 4.2 shows the velocity (color) for a range of Reynolds numbers and kinematic viscosities, if the vortex shedding frequency is taken to be $f_1$ = 0.63 Hz, the fundamental frequency of the harmonic tremor. The Reynolds number range for which vortex resonance occurs is indicated by cross-hatching. The colored bars show typical kinematic viscosities for dry air, water and steam at atmospheric pressure and various temperatures, for steam at 2x10$^7$ Pa and for andesite melt at several temperatures [MURASE and MCBIRNEY, 1973]. A lithostatic pressure $P$ = 2x10$^7$ Pa corresponds to a depth below the surface, $h$, of

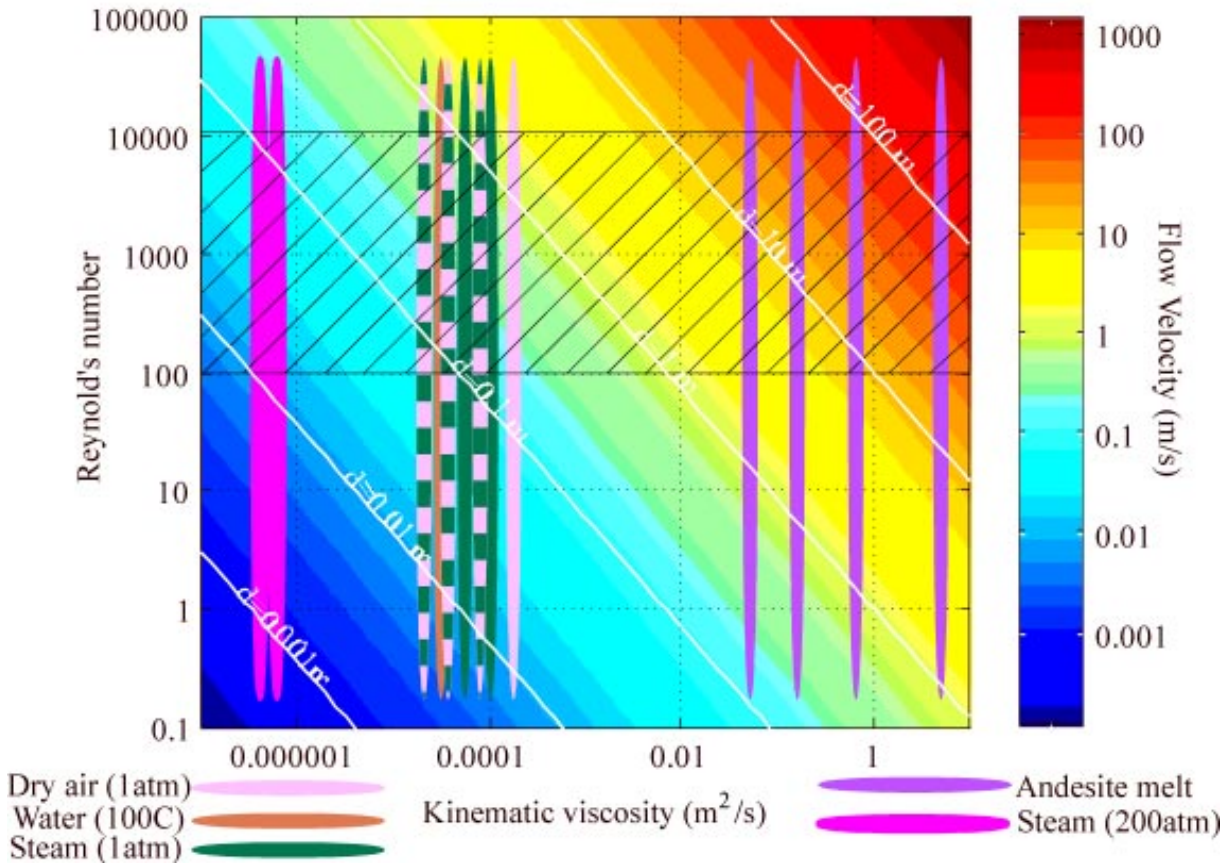


Figure 4.2 Flow velocities for the eddy shedding model as a function of Reynolds number and kinematic viscosity when the eddy frequency is 0.63 Hz. The flow velocity, denoted by color, is calculated from Equation 4.5. The colored bars give the kinematic viscosities of several fluids which may be encountered in a volcano. Eddy shedding may occur when the Reynolds number lies within the cross-hatched region. The white lines show the flow dimension as a function of kinematic viscosity and Reynolds number, given the eddy frequency.

$$h = \frac{P}{\rho g} = 2\text{x}10^7 \text{ Pa} / (2.5\text{x}10^3 \text{ kg/m}^3 \, 9.81 \text{ m/s}^2) \sim 800 \text{ m}$$

where ρ is the density of the rock and *g* the gravitational acceleration at the surface of the earth. Characteristic dimensions calculated using Equation 4.3, are plotted as labeled, white contour lines.

If vortex shedding resonance is the process which generates harmonic tremor, then Figure 4.2 provides several clues to the fluid involved, as well as the location and size of the obstacle causing the eddies. For steam at pressures equivalent to a depth of 800 m to shed eddies every 1.6 s, the obstacle could range in size from 4 mm to 4 cm at flow velocities of 1 cm/s to 10 cm/s. At the opposite end of the range of kinematic viscosity, even the most fluid andesite melt, assuming it retains the characteristics that MURASE and MCBIRNEY [1973] reported, must flow at 5 m/s to 50 m/s through characteristic flow dimensions of 5 m to 50 m in order to generate vortices that detach every 1.6 s. The order of magnitude for velocity and obstacle size for water at 100° C, superheated steam or dry air at atmospheric pressure are 0.1 - 5 m/s and 0.05 - 0.5 m, respectively. These dimensions are similar to those of dikes observed in volcanoes.

Shed vortices produce sound waves in two ways. First, the eddies produce density variations in the fluid, in particular when they come into contact with conduit walls, and are

Table 4 -- Eddy Shedding Forces

| Fluid | Density ($kg/m^3$) | Velocity (m/s) | Dimension (m) | Force assuming length of 1 m (N) |
|---|---|---|---|---|
| Steam ($2x10^7$ Pa) | 660 | 0.05 | 0.01 | 0.008 |
| Steam (100° C) | 0.6 | 1 | 0.5 | 0.15 |
| Steam (400° C) | 0.3 | 1 | 0.5 | 0.08 |
| Water (100° C) | 960 | 1 | 0.5 | 240 |
| Andesite (1400° C) | 2500 | 5 | 5 | $1.5x10^5$ |

therefore sources of sound waves. Secondly, each time an eddy is shed from the object, it produces a force on the object. The force per unit length due to shedding on a cylinder of diameter $d$, is given by MORSE and INGARD [1968]:

$$F_l \sim b\rho v^2 d/2, \qquad (4.6)$$

where where b is a unitless constant and its range, $0.5 \leq b \leq 2$, has been determined experimentally [MORSE and INGARD, 1968]. This force is similar to the force due to the Magnus effect. It is actually a time-varying force on the cylinder that increases as the vortex forms and reaches a maximum when the eddy is shed, then dropping suddenly. In the volcano, each impulse to the obstacle as an eddy is shed will propagate in the medium as a seismic wave. For the flow velocities and dimensions given in the previous paragraph, Table 4 gives

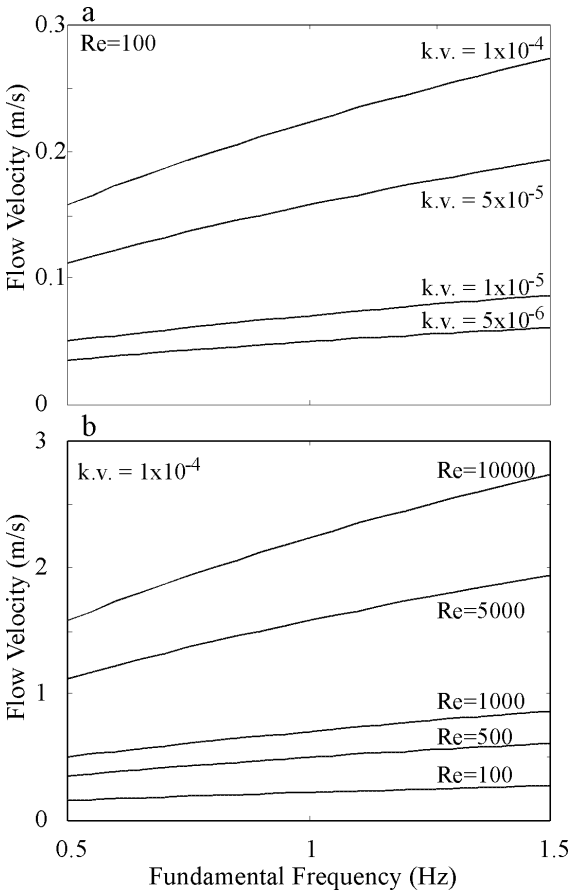


Figure 4.3 Relationship of flow velocity to frequency. (a) The Reynolds number is held constant and flow velocities are given for various kinematic viscosities taken from the range for air, steam and water at low pressures. (b) Kinematic viscosity is held constant and flow velocities are given as a function of shedding frequency for several Reynolds numbers. k.v. is the kinematic viscosity in $m^2/s$.

the force due to eddy shedding calculated using Equation 4.6 on a cylinder of 1 m length. These values can only be taken only as a rough estimate of the minimum order of magnitude for the force as they do not take resonance into account. This can intensify the force by several orders of magnitude. In addition, it is highly unlikely that the obstacle producing the eddies is a cylinder. While many papers describe observations and experimental evidence of damage due to eddy shedding, there are few measurements of the forces involved and little theory that can be applied to calculating exact forces. BLAKE [1986] reports that under appropriate geometric conditions, the forces due to eddy shedding can exceed the values predicted by Equation 4.6 by four orders of magnitude.

Section 3.1.2 gives the amplitude for a point force as the source of Lascar's harmonic tremor as being on the order of $10^6$ N. Even if feedback resonance is a factor [BLAKE, 1986], and the geometry of the vortex-producing obstacle can be approximated as a cylinder, so that Equation 4.6 is valid, it is unlikely that the first three substances listed in Table 4 would cause sufficiently large forces to be involved in the generation of harmonic tremor. According to the table, the forces due to the flow of andesite would be nearly large enough to produce the tremor observed at Lascar. It is, however, unlikely that andesite would flow at a velocity of 5 m/s or more, if the volcano is not erupting. There were no reports of eruptions during the observation of harmonic tremor. Only the vortex shedding in the flow of water near the surface, with the additional assumption of feedback resonance [BLAKE, 1986] produces forces which approximate the estimate of the amplitude of a point force derived from the seismograms using Equation 3.1.

If Lascar's harmonic tremor is caused by eddy shedding in a flow of hot water near the volcano's surface, changes in the frequency may result from changes in the flow velocity, the viscosity of the fluid or the geometry of the obstacle. If the geometry of the obstacle were to change rapidly, it would probably mean some movements of the rock walls of the conduit. Such changes are unlikely to be reversible and the tremor would probably stop. Reversible changes in the flow velocity, due to changes in the pressure or the kinematic viscosity are quite realistic. Figure 4.3a shows how the fundamental frequency changes with changing flow velocity at constant Reynolds number for several different kinematic

viscosities. In Figure 4.3b the relationship between flow velocity and frequency at various Reynolds numbers is shown for constant kinematic viscosity. Relatively large changes in the kinematic viscosity or the Reynolds number produce only small changes in the flow velocity and tremor frequencies.

## 4.2 Turbulent Slug Flow

Intermittent turbulence or turbulent slugs are sometimes observed in the transition from purely laminar pipe flow to completely turbulent flow [GINZBURG, 1963, TRITTON, 1988]. In this case, the slug is a region of turbulence in the pipe, which is separated from other turbulent segments by regions of laminar flow. Figure 4.4 shows a sketch of a slug flow cycle. If the reservoir is large, the pressure difference between the reservoir and the outlet will remain approximately constant over a long period of time. When calculating the Reynolds number for this experiment, the characteristic dimension is the diameter of the pipe or

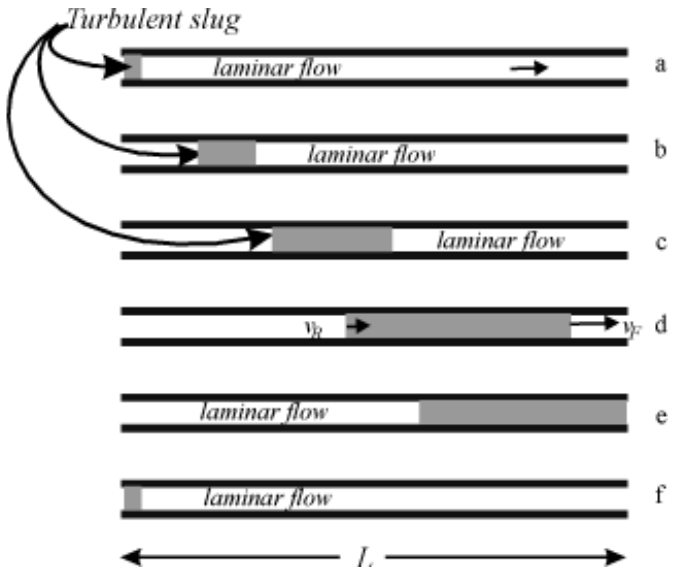


Figure 4.4 Cycle of turbulence slug generation. (a) Laminar flow in the conduit has reached a Reynolds number at which turbulence is generated at the intake. (b) The turbulence slows the flow and therefore lowers the Reynolds number, so that the fluid behind the turbulent section or slug again flows laminarly. (c-d) As the turbulent slug progresses through the conduit, it lengthens because its forward end progresses more rapidly than the average flow velocity while the rear end is slower. (e-f) Eventually the slug leaves the end of the conduit and the flow velocity increases again until a new slug is generated.

conduit, $d$. One of the necessary conditions for the generation of turbulent slugs is that the ratio of the length of the pipe or conduit, $L$, to its diameter, $d$, be $L/d > 50$. For a given pressure, the flow rate will be higher if the flow is laminar and lower if the flow is turbulent.

Imagine a situation, as in Figure 4.4, where the flow at a certain Reynolds number in a pipe connecting two reservoirs is laminar. Experiments have shown that sometimes when the Reynolds number increases, usually due to an increase in the flow velocity, turbulence develops at the intake (Figure 4.4a, [GINZBURG, 1963, TRITTON, 1988, FABER, 1995]). The turbulent slug moves through the pipe at a lower velocity than the laminarly flowing fluid (Figure 4.4b). At the same time, its front and rear edges propagate at different velocities through the pipe, the front at a higher velocity, $v_F$, than the "center" of the slug and the rear at a lower velocity, $v_R$, so that the slug grows in length as it progresses (Figure 4.4c). In the meantime, the fluid behind the slug can no longer flow at the high velocity which caused turbulence to develop; the flow becomes laminar again (Figure 4.4b). When the front end of the slug has left the pipe, the region of laminar flow grows until the rear of the turbulent slug has left the pipe (Figure 4.4e). Finally the velocity of the flow can again increase to the point at which a new turbulent slug is generated at the intake (Figure 4.4f). The cycle begins again.

The propagation velocities of the front and rear ends of the slug have been studied experimentally [TRITTON, 1988]. Figure 4.5 [taken from TRITTON, 1988] shows the ratios of $v_F$

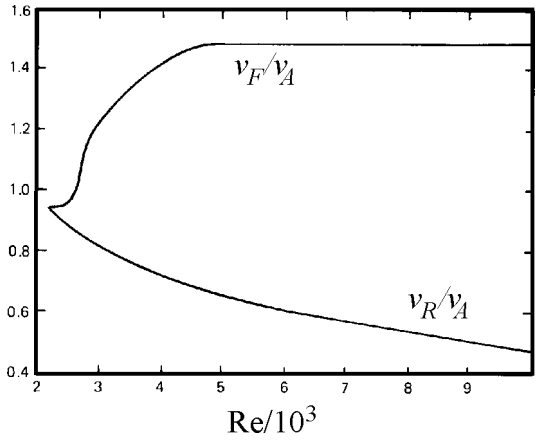


Figure 4.5 Ratios of front and rear velocities of turbulent slugs to the mean flow speed as functions of the Reynolds number, based on experimental results. Taken from TRITTON [1988], p. 286.

and $v_R$ to the mean flow velocity, $v_A$, as a function of the Reynolds number of the flow. When $Re$ ~ 2300 and generation of turbulent slugs begins, these two velocities are very close to $v_A$, and the slugs do not grow while flowing through the system.

Slug flow is a cyclic process. The period of the cycle is determined by the length of the conduit and the velocity of the rear of the slug,

$$T_S = L/v_R. \tag{4.7}$$

The flow leaving the conduit is turbulent from the time the front of the slug reaches the end, $L/v_F$, until the rear of the slug reaches the end, $L/v_R$. $T_T = L/v_R - L/v_F$ is the time the flow is turbulent. This value is used along with the cycle length to calculate the intermittency factor, the fraction of time that the motion is turbulent [TRITTON, 1988],

$$T_I = T_T/T_S = (L/v_R - L/v_F)v_R/L = 1 - v_R/v_F . \tag{4.8}$$

If, for a given configuration, the mean flow velocities in turbulent and laminar regimes are taken to be constants, and the change between the regimes virtually instantaneous, the variation of flow velocity can be modeled as a square wave (Figure 4.6a). This figure also shows the relationship between the intermittency and the period of the slug flow cycle. Figure 4.6b [TRITTON, 1988] shows an example of measured flow velocities taken from the

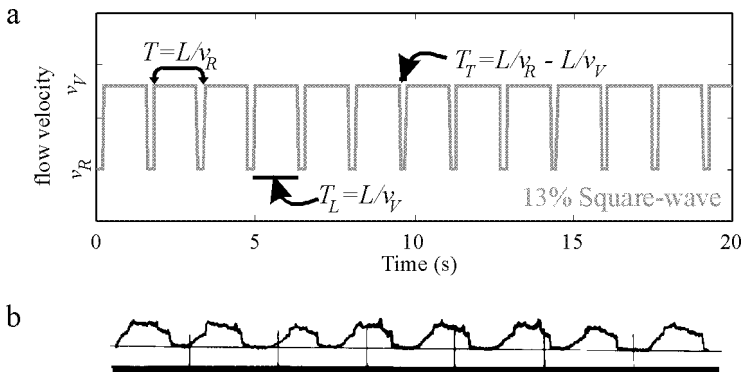


Figure 4.6 Flow velocity as a function of time in a fluid flowing in a turbulent slug regime. (a) Theoretical approximation using a 13% square wave describing the intermittency (Re=2675, taken from Table 5). (b) Trace of fluid velocity from a flow experiment showing local mean velocity changes between laminar and turbulent slug regimes (Re=5000, L/d=290). Taken from TRITTON [1988], p. 18.

literature. Although this waveform is not exactly a square-wave, this example does have extremely rapid velocity changes which produce harmonics in a Fourier spectrum.

For slug flow to occur in a volcano, two reservoirs of fluid must exist at different pressures, separated by a long, narrow conduit with $L/d > 50$ (Figure 4.7). Such conduits may be preserved as dikes often observed in eroded volcanoes. If the slug flow occurs in a conduit connecting an internal reservoir to the atmosphere and the volcano is not erupting, the fluid cannot be magma, but must be water or gases such as steam.

The parameters which define this model are the kinematic viscosity of the fluid, the pressure difference between the reservoirs and the dimensions (length and diameter) of the connecting conduit. To test the model, these parameters must be related to parameters which can be measured from the seismograms of harmonic tremor, such as the harmonic frequencies, $f_n$, $n$ = 1, 2, 3, ... (Figure 3.3), and the shape of the spectrum (Figure 3.5). Figure 4.8 shows the power spectrum of a 10 minute interval of harmonic tremor determined from the recording of the east component at station LA2. It is compared with the power spectrum of a 13% square-wave. These spectra are similar, in that their spectral lines appear in groups of 7, with decreasing amplitude. This suggests that the seismogram may be produced by a source function like a square wave with an intermittency of 13%. Figure 4.5 can be used to determine the intermittency for different Reynolds numbers (Table 5). For an intermittency of 13%, the Reynolds number of the flow is 2675.

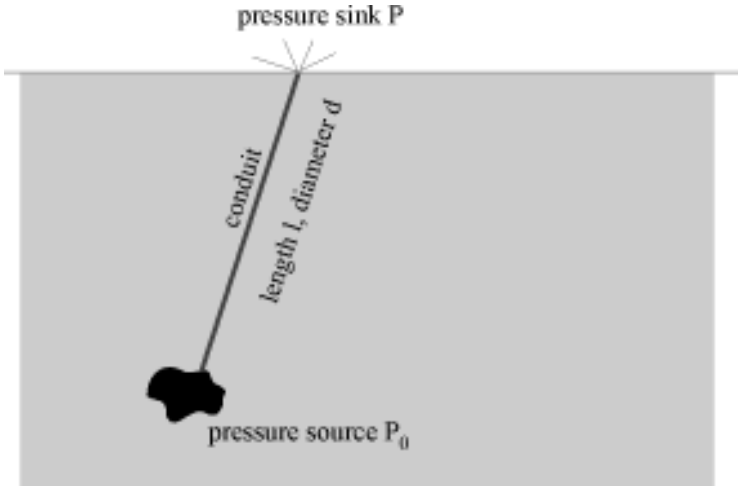


Figure 4.7 Geometry for generating turbulent slug flow in a volcano.

Table 5 -- Slug Velocities and Intermittancy

| $Re$ | $v_R$ | $v_F$ | Intermittency |
|---|---|---|---|
| 2300 | | | 0 |
| 2500 | 0.88 | 0.96 | 0.08 |
| 2675 | 0.87 | 1 | 0.13 |
| 2750 | 0.85 | 1.05 | 0.19 |
| 3000 | 0.8 | 1.22 | 0.34 |
| 4000 | 0.73 | 1.45 | 0.5 |
| 5000 | 0.65 | 1.48 | 0.56 |
| 6000 | 0.6 | 1.48 | 0.59 |
| 7000 | 0.55 | 1.48 | 0.63 |

According to this table and Figure 4.5, variations in the flow parameters should have two effects. The intermittency should change with the Reynolds number. In addition, the frequency of the cycle should change as the ratio of $v_R/v_F$ changes.

For a given Reynolds number, the flow velocity is related to the conduit size and the kinematic viscosity of the fluid by Equation 4.1. In Figure 4.9, the flow velocity has been calculated using Eq. 4.1 for $Re$ = 2675. The colors denote the flow velocity as in Figure 4.2.

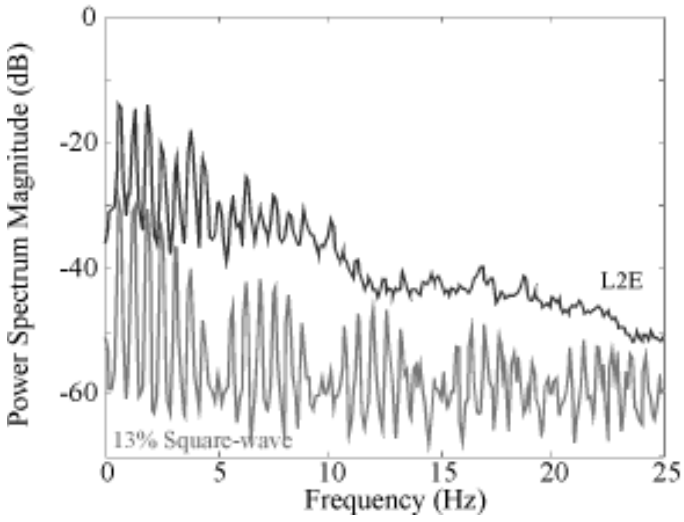


Figure 4.8 Comparison between the power spectra of harmonic tremor (black, taken from Figure 3.3b) and a 13% square wave (gray).

The cross-hatched area indicates the range of conduit sizes which may be expected in a volcano, while kinematic viscosities of andesite melt, water (100º C), steam at various temperatures and pressures, as well as dry air at several temperatures are marked for reference by colored bars.

Equation 4.8 gives another constraint on the geometry. If $L/d = 50$, as is necessary for slug flow and the period of the cycle is that of Lascar's harmonic tremor, $T_S = 1/f_1 = 1.6$ s, then $v_R = L/T_S = 50d/T_S = 50f_1d$. This is plotted in Figure 4.9 as a white bar marked with the frequency. It gives the correspondence between conduit size and flow velocity for cycles of $T_S = 1.6$ s. If the kinematic viscosity of the fluid is of the order of $10^{-6}$ m$^2$/s, as it would be for steam under high pressure, the conduit would be only several centimeters in diameter, and the flow velocity would be about 0.01 m/s. When the kinematic viscosity is about $10^{-3}$ m$^2$/s, in the range for air, water and steam at atmospheric pressure, which corresponds to near-surface hydrothermal activity, then the conduit diameter is on the order of 0.1 m and the flow velocity around 1 m/s. According to this model, the flow velocity for even the least viscous andesite melt is close to 100 m/s. Such movement is highly unlikely in a volcano that is not erupting. Thus, the slug flow model indicates that the source of the harmonic tremor recorded at Lascar Volcano must be near the surface, and the fluid generating the signals is not likely to be magma, but rather steam, water or air.

In a slug flow regime, the pressure at any given time and point along the conduit depends on whether the flow is mainly laminar or turbulent at that point. During laminar flow the pressure gradient is given by the Hagen-Poiseuille law [Schlichting, 1958, Faber, 1995]:

$$Re = \left(\frac{d}{2}\right)^3 \frac{\rho}{4\eta^2} \frac{dP}{dL}. \qquad (4.9)$$

Suppose one end of the conduit is at atmospheric pressure. If the dimensions for the conduit are taken from Figure 4.9 for flowing water as $d = 0.2$ m and the length is then calculated, $L = 50d = 10$ m, and the Reynolds number is 2675, then Equation 4.9 gives the pressure gradient as $dP/dL \sim 9$ N/m$^3$.

In the region of turbulence the pressure gradient will be steeper than where the flow is laminar, because the net movement of fluid through the conduit is lower than during laminar flow [Ginzburg, 1963, Tritton, 1988, Faber, 1995]. When the flow is fully turbulent, the Reynolds number and the pressure gradient are related by an experimental relationship given by Blasius [Schlichting, 1958, Faber, 1995]

$$Re^{7/8} = \frac{22.4}{\pi}\left(\frac{\rho(d/2)^3}{\eta^2}\frac{dP}{dL}\right)^{1/2} . \qquad (4.10)$$

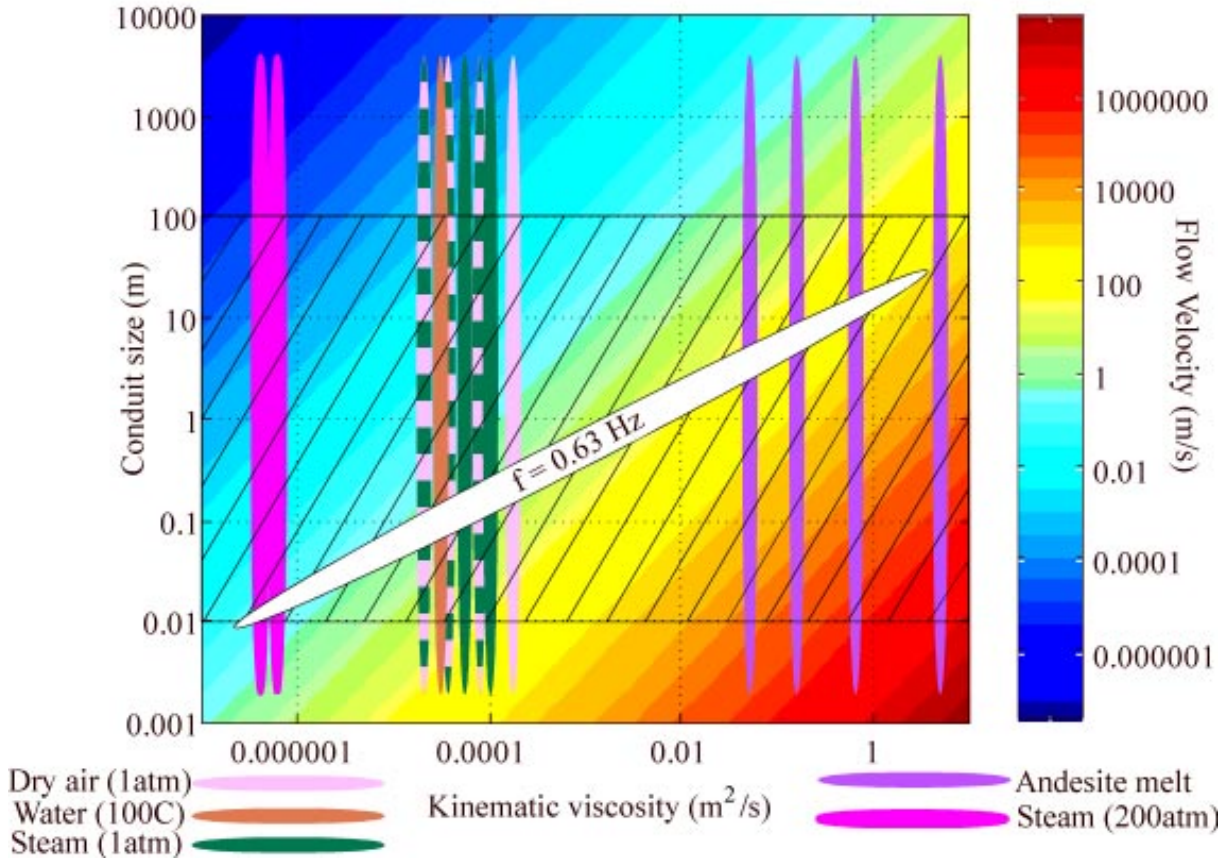


Figure 4.9 Flow velocities for the slug flow model as a function of conduit size and kinematic viscosity when the Reynolds number of the flow is 2675. The flow velocity, denoted by color, is calculated using Equation 4.1. The colored bars give the kinematic viscosities of several fluids which may be encountered in a volcano. Conduit diameters may be reasonably expected to lie within the cross-hatched region. The sloped white region shows configurations for which the slug flow cycle would have a period of $T_S = 1/f_1 = 1.6$ s.

For the same geometry and Reynolds number as above, the pressure gradient is $dP/dL$ ~ 16 N/m$^3$ for turbulent flow.

In this model, the harmonic tremor signal measured at the stations of the Lascar network is caused by changes in the fluid's pressure which occur when the flow changes from laminar to turbulent. In principle, these pressure variations act as a variable force on the conduit walls [Wallis, 1969, Chouet et al, 1997]. Unfortunately, it is difficult to describe these variations theoretically. Although the description here gives the Reynolds number as a constant, it in fact changes during a cycle as the flow changes from laminar to turbulent and back (Figure 4.10). Practically it is difficult to estimate the relative volumes and flow velocities of laminar and turbulent fluid as a function of the cycle. In addition, as shown in Figure 4.10, experiments have demonstrated that Equations 4.9 and 4.10 do not completely describe situtations in which intermittent turbulence and slug flow develop, because the flow is not completely turbulent [Schlichting, 1958]. It is thus difficult to correctly estimate the amplitude of the forces on the medium during slug flow.

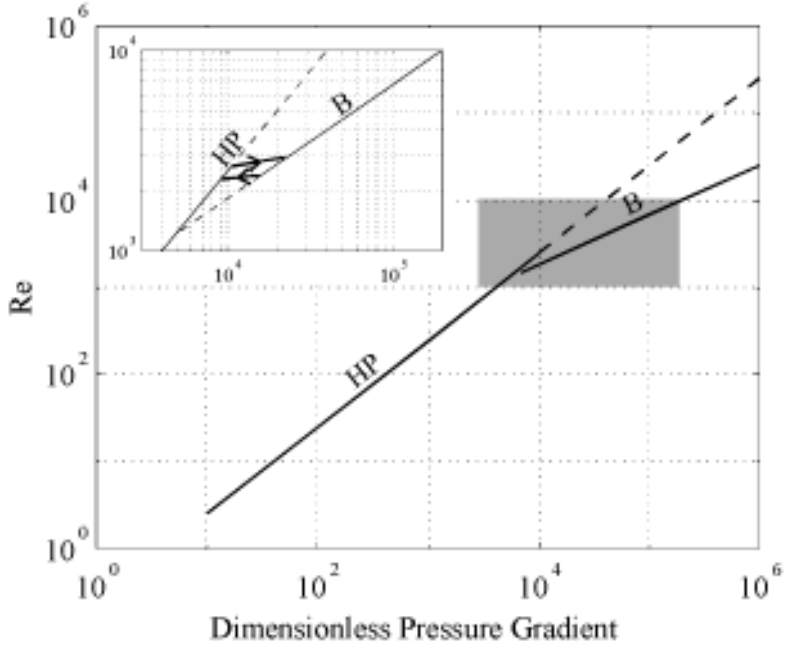


Figure 4.10 Reynolds number as a function of pressure gradient for pipe flow. HP marks the Hagen-Poiseuille relationship for laminar flow while B marks the Blasius relationship for fully turbulent flow. The inset shows approximately how the Reynolds number and pressure gradient change during slug flow.

On the other hand, a simple estimate of these forces can be made by calculating the change in the fluid's momentum between the laminar and turbulent flow regimes. Several assumptions are necessary. If the conduit is assumed to be completely filled with either laminarly or turbulently flowing fluid with the transition between the two regimes occurring in 0.001 s, and if the compressiblity of the fluid is neglected, then Table 6 gives the change in fluid momentum, $\Delta p$, for several different fluids. These values are calculated for a Reynolds number of 2675 and a fundamental frequency of $f_1$ = 0.63 Hz. In addition, Table 6 gives the conduit dimensions and fluid density and velocity for these flow parameters. The change in momentum of the fluid in the conduit is the force on the fluid in remaining in the reservoir. In this case, only water produces a force comparable to the values of $3.2 \times 10^6$ and $1.1 \times 10^6$ N determined for harmonic tremor in Section 3.1.2. If the transition is assumed to occur slowly in 0.2 s, the interval given by the intermittancy, the forces are much smaller (Table 6).

Table 6 -- Slug Flow Forces

| Fluid | Density ($kg/m^3$) | Conduit Diameter(1) (m) | Conduit Length(2) (m) | Velocity(3) (m/s) | Mass of Fluid (kg) | $\Delta p$(4) (N) | $\Delta p$(5) (N) |
|---|---|---|---|---|---|---|---|
| Water (100° C) | 1000 | 0.35 | 17 | 11 | 1600 | $2.6 \times 10^6$ | $1.3 \times 10^4$ |
| Air ($1 \times 10^5$ Pa, 100° C) | 0.9 | 0.32 | 16 | 10 | 1.2 | 1800 | 9 |
| Air ($1 \times 10^5$ Pa, 300° C) | 0.6 | 0.46 | 23 | 14 | 2.3 | 4900 | 24 |
| Steam ($1 \times 10^5$ Pa, 100° C) | 0.6 | 0.3 | 15 | 9.5 | 0.6 | 900 | 5 |
| Steam ($1 \times 10^5$ Pa, 300° C) | 0.4 | 0.48 | 24 | 15 | 1.6 | 3600 | 18 |
| Steam ($2 \times 10^7$ Pa, 300° C) | 7 | 0.11 | 6 | 3.5 | 0.4 | 200 | 1 |

(1) Calculated from $Re = vd/\kappa$, with $Re$=2675, $v = d f_1$ and $f_1$ = 0.63 Hz
(2) Calculated from $L/d$=50
(3) Velocity during laminar flow
(4) Calculated assuming fluid velocity drops by 15% due to turbulence in 0.001 s
(5) Calculated assuming fluid velocity drops by 15% due to turbulence in 13% of one period or 0.2 s

## 4.3 Soda Bottle

When a system such as a volcano is closed to the atmosphere, the liquids, either magma or water in the hydrothermal system, must be saturated with gases. When such a system opens rapidly, the rapid and explosive degassing which takes place is usually a volcanic eruption or explosion. If, on the other hand, the opening is very small, the gases can only escape slowly. This may give rise to a cycle of pressure drop and bubble formation which can often be observed when a bottle of carbonated water is opened slightly [SOLTZBERG, 1997]. Similar cycles have also been observed in the slow decompression of more viscous fluids used to model volcanic systems [HAMMER et al, 1998]

Figure 4.11 shows a series of pictures taken of a bottle of soda water after its cap was opened only a small amount. Initially, the gas escapes slowly with a hissing noise, and the gas pressure in the volume above the water decreases. When the pressure has dropped enough to overcome the bubble surface tension [LEIGHTON, 1994, SOLTZBERG et al, 1997], bubbles form throughout the water. Their presence compensates for the initial decrease in pressure and therefore inhibits the formation of more bubbles. While gas continues to escape through the “vent” in the cap, the existing bubbles rise toward the surface during an interval which depends on the size (depth) of the bottle. When all the bubbles have reached the surface they can no longer contribute to the pressurization of the bottle, so the pressure again drops as gas continues to escape. When the pressure has dropped enough to overcome the bubble surface tension, the cycle begins again.

Figure 4.11 Photograph series of bubble cycle in a slightly opened bottle of soda water. On the left, the bottle has just been opened. Time increases toward the right.

A similar situation may exist in a volcano, where a small vent or opening allows gas to escape slowly. The volcano's reservoir of gas-saturated magma or water is large, and may, for the purposes of a simulation, be considered to provide an endless supply of gas when the pressure drops below the saturation level. In such a case, the soda bottle cycle could continue for hours.

To describe the processes in the slightly opened soda bottle quantitatively several assumptions are necessary. Figure 4.12 shows schematic pictures of the soda bottle during an interval when there are no bubbles and at a later point in the cycle when bubbles have formed. The gas, particularly at high temperatures such as would be expected in a volcano, may be described using the ideal gas law [GERTHSEN et al, 1974]

$$PV = NRT\,, \tag{4.11a}$$

where $P$ and $V$ are the pressure and volume of $N$ moles of ideal gas at temperature $T$. $R$ is the universal gas constant. If the number of moles is rewritten as the quotient of the total mass of the gas divided by its molecular mass, $m/M_{gas}$, this equation becomes

$$PV = \frac{R}{M_{gas}} mT = mR'T\,, \tag{4.11b}$$

where $R$', the universal gas constant, has been normalized by $M_{gas}$. The mass of the gas divided by its volume is its density, ρ, giving the relationship

$$P = \rho R'T \tag{4.11c}$$

From Equation 4.11b, the time derivative of the mass flux may be written as

$$R'T\dot{m} = \dot{p}V + p\dot{V}\,. \tag{4.12}$$

If we assume that the volume of the fluid present does not change, then the total volume filled with gas also remains constant, so that $V = V_0$ and $\dot{V} = 0$. As is to be expected, changes in the pressure in the gas-filled region depend on the mass flux

$$\dot{P} = \frac{R'T}{V_0}\dot{m} = \frac{R'T}{V_0}\left[\dot{m}_e + \dot{m}_b\right] \ . \qquad (4.13)$$

Two factors contribute to the mass flux, gas escaping from the volume through the vent and gas leaving the liquid in the form of bubbles. The mass flux of escaping gas, $\dot{m}_e$, is the product of the density of the gas, ρ, times the cross-sectional area of the vent, $q$, and the velocity of the gas, $v$. The mass flux of gas entering the gas-filled volume from bubbles, $\dot{m}_b$ ,can be described by product of the mean density of bubbles,

$$\bar{\rho}_b = n_b\left\langle \frac{4\pi}{3} r_b^3 \rho_{gas} \right\rangle \ , \qquad (4.14)$$

with the cross-sectional area of the liquid, $Q$, and the mean ascent velocity of the bubbles, $\bar{v}_b$ . In Equation 4.14, $n_b$ is the number of bubbles per unit volume, and the factor in brackets is the mean bubble mass, calculated from the volume of spherical bubbles of radii $r_b$, and their density, $\rho_{gas}$.

The change in pressure as a function of time is then

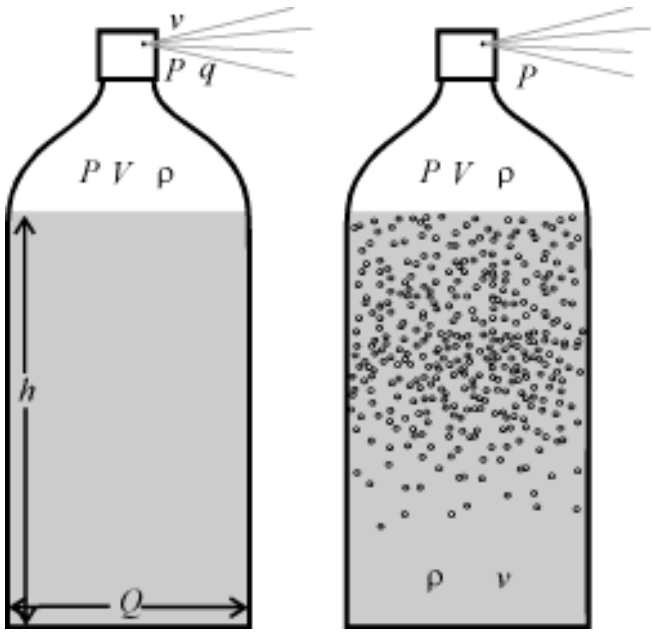


Figure 4.12 Sketch of soda bottle showing parameters used in Equations 4.11 - 4.21.

$$\dot{P} = \frac{R'T}{V_0}\left[\dot{m}_e + \dot{m}_b\right] = \frac{R'T}{V_0}\left[-\rho q v + \bar{\rho}_b Q \bar{v}_b\right] \tag{4.15}$$

It is not unreasonable to assume that the geometric parameters, such as $Q$ and $q$, remain constant over several degassing cycles in a soda bottle or a volcano. Further, we may assume that the velocity of the escaping gas, $v$, is proportional to the difference in pressure between the interior of the bottle or volcano and the outside, with a proportionality constant $k'$ [GINZBURG, 1963]

$$v = k'\left(P - P_a\right). \tag{4.16}$$

Inserting these values into Equation 4.15 and using Equation 4.11c for the density of the gas, gives a non-linear differential equation for the pressure:

$$\dot{P} = -\frac{qk'}{V_0}P\left(P - P_a\right) + \frac{R'TQ}{V_0}\bar{\rho}_b\bar{v}_b = -\frac{qk'}{V_0}P^2 + \frac{qk'P_a}{V_0}P + c_b = \quad . \tag{4.17}$$

$c_1 = qk'/V_0$, and $c_2 = c_1 P_a$ are constants for the soda bottle, and may vary slowly as a function of time in a volcano. If the bubbles rise with constant velocity the final parameter,

$$c_b = \frac{R'TQ}{V_0}\bar{\rho}_b\bar{v}_b, \tag{4.18}$$

may be related to the kinematic viscosity of the liquid by setting Stoke's law equal to the bubbles' bouyancy and and solving for the velocity .

$$c_b = \frac{R'TQ}{V_0}\bar{\rho}_b\frac{2\pi\bar{r}_b^{\,2}g}{9\kappa}, \tag{4.19}$$

Thus, $c_b$ is inversely proportional to the kinematic viscosity of the liquid.

In fact, $c_b$ is non-zero only if bubbles are present, since $\bar{\rho}_b$ is proportional to $n_b$, the number of bubbles per unit volume. The presence of bubbles depends on the bubble

nucleation rate. According to SOLTZBERG et al [1997], the bubble nucleation rate, $\dot{n}_b$, is an exponential function of the Helmholtz energy, $\Delta E_H$, necessary to form a bubble,

$$\dot{n}_b \propto \exp(-\Delta E_H / kT), \tag{4.20}$$

where $k$ is Boltzmann's constant and $T$ is the temperature. From classical nucleation theory, the Helmholtz energy is proportional to the cube of the bubble surface tension, $\sigma_S$, and inversely proportional to the square of the difference between the supersaturation concentration of disolved gas in the fluid, $c_S$, and the equilibrium concentration, $c_{eq}$. Using Henry's law, $c = \mathrm{K}P$, these concentrations can be used to relate the Helmholtz energy to the original pressure in the system, as well as, the pressure after it drops,

$$\Delta E_H = 16\pi\sigma_S^3 \mathrm{K}^2 / 3(c_S - c_{eq})^2 = 16\pi\sigma_S^3 / 3(P_S - P_{eq})^2 . \tag{4.21}$$

For the soda bottle, $P_S$ is the initial pressure of gas in the bottle. Bubbles begin to form when $P_{eq} = 2\sigma_S/r_b$, that is, when it reaches the Laplace pressure corresponding to the surface tension in a bubble of radius $r_b$.

Initially, there are no bubbles in the bottle, $n_b \sim 0$. According to Equation 4.20, $\dot{n}_b$ is very small and nearly constant until $P_S \sim P_{eq}$, when it very suddenly becomes extremely large. Thus, no bubbles appear spontaneously until the pressure drop exceeds the Laplace pressure. They immediately cease to form as soon as $P_{eq}$ rises again due to the presence of bubbles.

To simplify calculations, Equation 4.17 can be solved for two cases. I assume $c_b = 0$ initially when no bubbles are present, and after a wave of them has risen to the surface. It is a non-zero constant depending on the viscosity of the liquid, on the bubble density and rise velocity, and on the geometry of the chamber when bubbles are present. In this case, bubble formation acts as a regulator relay for the self-regulation of the pressure in the bottle or volcano [MAGNUS and POPP, 1997]. Equation 4.17 can be solved numerically, using Matlab, for example. Figure 4.13 shows several solutions for assumed initial conditions in a soda bottle. As $c_b$ increases, that is with decreasing kinematic viscosity of the liquid, the bubbles rise more quickly and pressure oscillations increase dramatically in amplitude. To

produce the oscillations observed at Lascar, with a fundamental frequency of 0.63 Hz, the kinematic viscosity of the liquid involved must be low. It could, for example, be water near the surface at relatively low overpressure.

Although this description of the soda bottle phenomenon is highly simplified, the model generates non-sinusoidal waveforms (Figure 4.13) which resemble the seismograms of harmonic tremor at Lascar. They are produced by pressure variations inside the reservoir during the bubble formation cycle. Under the simple assumptions used for solving Equation 4.17, the pressure changed by more than a factor of 2.

ACHENBACH [1975] gives a relationship describing the wavefield generated by pressure changes in a spherical cavity of radius *A* in a homgeneous, isotropic and linearly elastic medium. If the pressure change is a step function, $P(t) = P_0 H(t)$ with $H(t)$ the Heaviside function, then the displacement potential is

$$\Phi(r,t) = -\frac{1}{4\mu}\frac{A^3 P_0}{r}[1-(2-2\sigma)^{1/2}\exp(-\chi s)\sin(\varphi s+\lambda)]H(s \qquad (4.22)$$

where $\alpha$ is the speed of longitudinal waves in the medium, $\sigma$ is the Poisson ratio, $\mu$ is the shear modulus, $\chi$, $\varphi$ and $\lambda$ are defined as

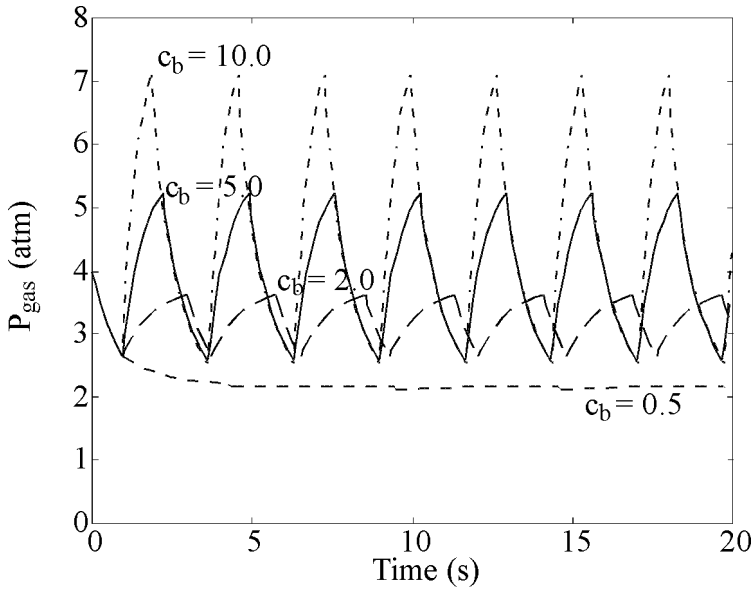


Figure 4.13 Pressure oscillations in a soda bottle with a small opening. The curves are marked with their initial conditions.

$$\chi = \frac{1-2\sigma}{1-\sigma}\frac{\alpha}{A}, \quad \varphi^2 = \frac{1-2\sigma}{(1-\sigma)^2}\frac{\alpha^2}{A^2}, \quad \lambda = \cot^{-1}(1-2\sigma)^{1/2} \quad (\pi/4 \le l \le \pi/2)$$

and

$$s = t - \frac{r-a}{c_L}.$$

A pulse of finite duration, $\tau$, can be simulated by superimposing the displacement potential for a pressure change of equal but opposite magnitude a time $\tau$ after the initial pressurization. Solutions for Equation 4.22 giving the displacement at a distance $r$ = 4000 m, using $\alpha$ = 1000 m/s, $\sigma$ = 0.3 and $\mu$ = 2x10$^{10}$ N/m$^2$ are plotted in Figure 4.14. The expected displacement is displayed as a function of the source radius, $A$, for initial pressures, $P_0$ = 3 atm, 5 atm and 7 atm, the pressures used in the calculations for Figure 4.13. The root mean square displacement measured at LA2 is also plotted as a dashed line. It intersects the lines for all three atmospheric pressures at a radius of about 20 m. This indicates that

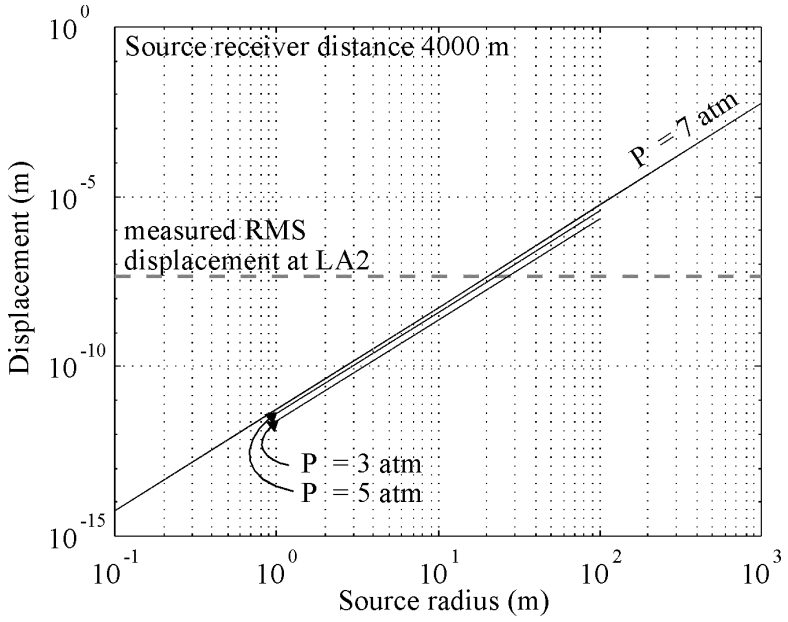


Figure 4.14 Displacement amplitude due to a pressure pulse at 4000 m distance from a spherical cavity of radius $A$ in a homgeneous, isotropic and linearly elastic medium calculated using Equation 4.22. The dashed line is the root mean square displacement amplitude measured at station LA2. The solid lines are for pressure differences between the interior of the sphere and the environment of 3 atm, 5 atm and 7 atm.

under the simplifying assumptions used here, fluctuating pressure of the order of magnitude described above in a sphere with a radius of 20 m, or approximately $3x10^4$ $m^3$ volume, could produce the harmonic tremor seismograms measured at Lascar. If harmonic tremor is produced by such a mechanism, Lascar must contain such a volume of boiling or otherwise periodically degassing fluid.